Simulation of physicochemical processes of dissolution, transport, and deposition of gold in epithermal Au-Ag deposits in northeastern Russia

Article *in* Geologiya i Geofizika · January 2001

CITATIONS
17

READS
22

4 authors, including:

K. V. Chudnenko
Russian Academy of Sciences
100 PUBLICATIONS **968** CITATIONS
SEE PROFILE

R. G. Kravtsova
Vinogradov Institute of Geochemistry SB RAS
66 PUBLICATIONS **282** CITATIONS
SEE PROFILE

Valeriy A Bychinsky
57 PUBLICATIONS **479** CITATIONS
SEE PROFILE

ISSN 1068-7971

RUSSIAN GEOLOGY AND GEOPHYSICS

ГЕОЛОГИЯ И ГЕОФИЗИКА

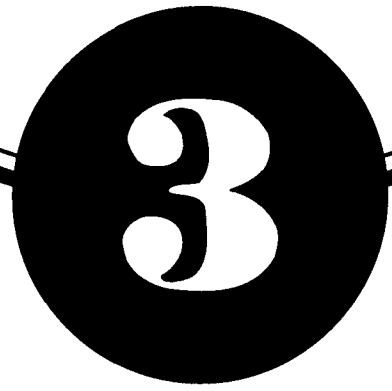

Vol. 42, 2001

Allerton Press, Inc. / New York

Russian Geology and Geophysics
Vol. 42, No. 3, pp. 379-394, 2001

Geologiya i Geofizika
UDC 550.8.013+550.42(571.65)

SIMULATION OF PHYSICOCHEMICAL PROCESSES OF DISSOLUTION, TRANSPORT, AND DEPOSITION OF GOLD IN EPITHERMAL Au-Ag DEPOSITS IN NORTHEASTERN RUSSIA

I. K. Karpov, K. V. Chudnenko, R. G. Kravtsova, and V. A. Bychinskii

Institute of Geochemistry, Siberian Branch of the RAS, ul. Favorskogo 1a, Irkutsk, 64033, Russia

Water-bearing fluids are supposed to result from thermodynamically equilibrated andesite–water interaction in a zone of accumulation of hydrothermal solutions from peripheral magma chambers. Thus, intermediate magma chambers, derivates of the primary andesite magma, are assumed to exist. As a result of the interaction, Au and Ag, which are found in andesites and rhyolites in clarke concentrations, are mobilized into a fluid phase with Au increased by a factor of 200–500 and Ag, by a factor of 100–200. In addition, meteoric waters, percolating to the root zone of the hydrothermal block through andesites and coming to the surface through fissure channels, cannot be a potential source of Au epithermal deposits. However, "empty" Au hydrotherms of meteoric origin can participate in redistribution and remobilization of the earlier deposited gold, bringing it to the surface at the final stage of evolution of a hydrothermal system. The main mode of occurrence of dissolved Au is hydrosulfide $Au(HS)_2^-$. Chloride complexes of Au are subordinate no matter which rock (andesite or rhyolite) is in equilibrium. Silver occurs both as chlorides and as hydrosulfides. However, chlorides are predominant in the rhyolite fluid.

Gold, epithermal hydrothermal deposits, simulation of physicochemical processes

BACKGROUND

Although for the last 20–25 years Russian and foreign researchers were quite successful in constructing a quantitative theory for endogenous fluid systems, this problem is far from being solved. It is hardly possible to create a universal model for the formation and development of hydrothermal systems, but we can develop quantitative schemes for the evolution of a finite number of basic structural and dynamic types of fluid-magmatic systems, modeling the processes which govern dissolution, transport, and deposition of ore and petrogenic elements. This compositional approach proposed by Sharapov [1] may be useful in solving particular problems of hydrothermal ore formation. It permits recognition of a standard part in them, which can be treated by means of reference models, available algorithms, computational schemes and programs, and a nonstandard part, related to the specific character of a given geologic object. Taking this into account, we can reconstruct both a general picture and particular features of evolution of a certain hydrothermal system, using the available schemes, algorithms, and procedures.

Progress in this field will depend on imitation modeling [2]. Combined with qualitative geological and geochemical constructions, analytical and numerical solutions to problems of heat and mass transfer, imitation modeling appears to be the only appropriate means for investigating specific features of hydrothermal systems in a physicochemical process of their origin, development, and extinction. Of principal importance is the following fact. When we turn our attention to the most complete physicochemical presentation of natural processes, even relatively simple models with participation of aqueous (fluid) solutions of electrolytes inevitably make us add individual substances (dependent components after Gibbs) to the initial multisystem. We refer to large and permanently expanding bases of thermodynamic data on dependent components of aqueous (fluid) solutions of electrolytes on the basis of a modified HKF equation of state [3–10]. The list of the substances

which potentially can be in equilibrium becomes even longer if a gas mixture coexists with the aqueous solution. The application of methods of free energy minimization considerably extended the potentialities of modeling of real conditions without significant physicochemical reduction of input data, unavoidable in reaction-based modeling. Thus, Grichuk et al. [11], Borisov and Shvarov [12] solve problems related to the water-rock interaction in hydrothermal systems as part of an extended multisystem with 15 independent components. The initial list contains minerals and aqueous solution of electrolyte, but it does not include a gas phase potentially possible in an equilibrium composition. This exclusion, connected with characteristics of the algorithm used [13], certainly restricts the potential of the imitation method, since the appearance or disappearance of gas phase, leading to a dynamic change in the aqueous solution–gas mixture, is one of the main factors of hydrothermal ore formation.

This paper is aimed at reaching two goals. First, using a sufficiently simple example, we will show how it is possible to construct an imitation model for a hydrothermal system with participation of minerals, aqueous solution of electrolyte, and gas phase, with a set of reservoirs connected with one another and with the environment through flows of mobile groups of phases [2, 14]. This example is so illustrative that the idea can be grasped at first glance, without getting into the technical details. Thus, we outline the contours for the application of the new approach to study hydrothermal ore formation by imitation modeling using the Selektor-C program complex [2, 15, 16]. The second goal is to disclose the technique of model formation and numerical experiments: determination of initial conditions and restrictions, recognition of reservoirs and flows connecting them into a single dynamic megasystem, description of processes, and analysis of imitation results. To illustrate this, we took a generalized model reflecting the most typical features of dissolution, transport, and deposition of gold in epithermal gold-silver deposits which formed under the conditions of typical continental margins of northeastern Asia on the basis of Kravtsova's data.

INPUT DATA OF MODEL

Geological exposition. The gold-silver deposits of the Eveny volcanic zone, a constituent of the Okhotsk-Chukchi volcanic belt, formed under the conditions of open volcanogenic-hydrothermal systems, in which the fluid flows from deep sources are connected with the Earth's surface [17]. According to Sharapov's classification [1], these are volcanogenic-hydrothermal systems of the onland regions of active volcanism. The deposits under study are of vein type and have all geological and mineralogical characteristics of near-surface epithermal sulfide-poor gold-silver formation [18]. The structural-geological position of the deposits is described by Belyi [19], Terekhov [20], and Umitbaev [21]. Orebodies and syngenetic metasomatites are confined to systems of fractures feathering deep faults. The composition of orebodies is as follows: quartz, K-feldspar (adular), sericite, hydromicas, carbonate, kaolinite, and ore minerals. The commonest ore mineral is pyrite. There are also argentite, gold, electrum, sulfosalts of silver, and other ore minerals. Wallrock metasomatites are intimately connected with ore zoning and rest upon regionally propylitized rocks.

Three types of metasomatic columns develop upon the propylitized rocks: quartz-adular, quartz-sericite, and quartz-hydromica. The sequence of mineral zones in the three types of columns is quite similar. The frontal zone is ore-adjacent propylite, rear zones are quartz in quartz-sericite or quartz-hydromica columns and quartz-feldspar or feldspar in the quartz-adular-type metasomatites. Intermediate zones show various ratios of quartz, sericite, hydromicas, pyrite, chlorite, albite, and carbonate, with one additional mineral in paragenesis in each subsequent zone (from rear to frontal). Thus, the structure of the metasomatic columns indicates that their formation occurred by infiltration mechanism of water-rock interaction [22, 23].

Formation of imitation model of a hydrothermal system. At present, a generalized image of a hydrothermal ore-forming system is widely used. Its components are: magma chamber or, without further detail, deep-seated source of heat and/or volatiles; unidirectional upward flow of volatiles from the deep-seated source at a near-lithostatic pressure; upper, reaching the Earth's surface, block of enclosing rocks disintegrated and deconsolidated to different degrees, in which ascending and descending flows of deep and meteoric infiltration waters circulate under hydrostatic pressure; passing through the hydrothermal overburden, fluid channels from below-ore sources to surface are geologically documented in the form of different deep fractures and fractured zones whose permeability is an order as high as the volume permeability of the disintegrated block of enclosing rocks. Various researchers individualize this image, reflecting their own understanding of geological and geochemical features of particular types of the deposits under study. Although each author creates, materially or mentally, his or her own picture of fluid ore-forming systems in a specific fashion and with particular details, a single common scheme is tentatively outlined in the diversity of proposed versions. This is also visible in our sketch (Fig. 1) presenting a generalized scheme of a multireservoir thermodynamic

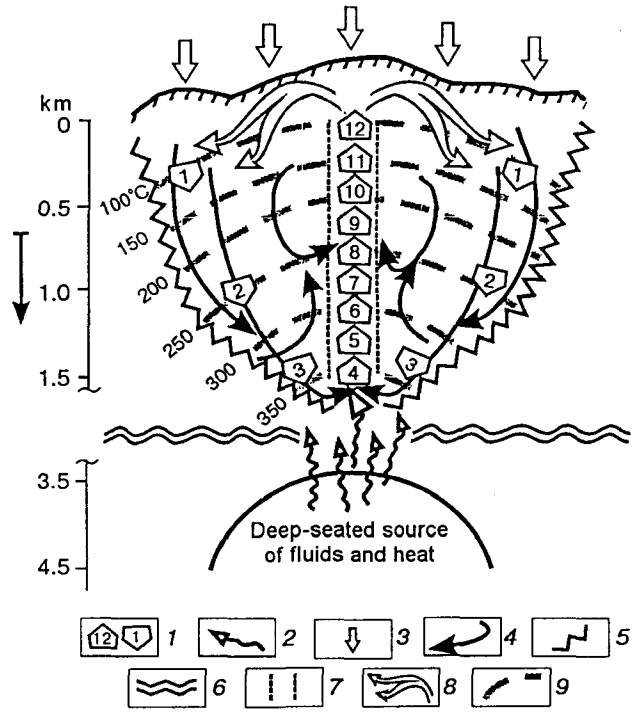

Fig. 1. Generalized scheme of multireservoir thermodynamic model of volcanogenic-hydrothermal ore-forming system of epithermal gold-silver deposits in northeastern Asia. 1 – numbered reservoirs; 2 – ascending flow of deep-seated fluid; 3 – meteoric waters; 4 – descending flow of infiltration waters; 5 – boundaries of hydrothermal system; 6 – boundary separating the region of hydrostatic pressure from the lower region with predominant lithostatic pressure; 7 – fractured channel through which ascending flows of hydrothermal solutions transit; 8 – discharge of hydrothermal solutions in the regime of dissipation and spreading; 9 – isotherms.

model of a volcanogenic-hydrothermal ore-forming system of epithermal gold-silver deposits of northeastern Asia. Estimates of temperature, pressure, and depth agree with data by Gumenyuk and Gundobin [24], Gundobin and Kravtsova [25], Kravtsova [26–28], as well as with data on hydrothermal systems of similar nature [29–33].

Chemical composition of enclosing rocks. The chemical and trace-element composition of the Upper Cretaceous effusive and ore-associated intrusive rocks enclosing the gold-silver mineralization in the region under study and their potential mineralization are considered in detail by Zakharova and Kravtsova [34, 35]. Medium chemical compositions of these igneous rocks (andesites, rhyodacites, and granodiorites) recalculated to molar amounts of elements in 1 kg of rock are given in Table 1.

DIMENSIONS OF THE HYDROTHERMAL SYSTEM

The vertical extension is taken to be equal to 1.5 km and both width and length are 4 km. The volume of the entire deconsolidated block is: $1.5 \times 4 \times 4 = 24$ km^3 or $24 \cdot 10^9$ m^3. Assuming that the density of the enclosing rocks is 2.7 tons/m^3, we obtain the weight of the entire hydrothermal building, $64 \cdot 10^9$ tons. The fractured zone is extended depthward for 1.5 km; its length is 4 km, and width, 0.02 km. Its volume is $12 \cdot 10^7$ m^3 and weight is $32.4 \cdot 10^7$ tons. Thus, the fractured zone occupies 0.5 vol.% of the hydrothermal system.

Flow of deep-seated fluids. Mathematical modeling of degassing of a magma chamber about 50 km^3 in volume, filled with a melt [36, 37] of acid composition in the process of its crystallization, shows that the velocity of the fluid flow during the convective stage is estimated at $7 \cdot 10^5 - 1.5 \cdot 10^6$ tons/year, which is comparable with the velocity of passive discharge of high-temperature volatiles (>700 °C) in active volcanic systems of the Pacific-framing volcanic belt [30, 38, 39]. Shinohara and Hedenquist [37] recognize two stages of degassing of a deep-seated source. In the first, relatively short, stage the melt is convectively mixed in the

Table 1

Mean Compositions of Rocks of Ore-Bearing Volcanotectonic Structures in Central Part of the Okhotsk-Chukchi Volcanonogenic Belt Recalculated to Molal Amounts of Elements in 1 kg of Rock

Independent component	Andesite, n = 120	Rhyolite and rhyodacite, n = 106	Granite, granodiorite, n = 50
K	0.386	0.8642	0.7664
Na	1.11	1.1248	1.17452
Ca	1.159	0.2377	0.47026
Mg	0.8088	0.0941	0.2662
Fe	1.0347	0.3317	0.5194
Al	3.424	2.7274	2.9778
Si	9.335	12.237	11.24958
Au	$1.2\cdot10^{-8}$ ($2.8\cdot10^{-8}$)[a]	$0.8\cdot10^{-8}$ ($2.8\cdot10^{-8}$)[a]	$1.5\cdot10^{-8}$ ($2.8\cdot10^{-8}$)[a]
Ag	$1.464\cdot10^{-6}$ ($3.559\cdot10^{-6}$)[b]	$1.779\cdot10^{-6}$ ($3.559\cdot10^{-6}$)[b]	$1.288\cdot10^{-6}$ ($3.559\cdot10^{-6}$)[b]
S	0.0605	0.01101	0.00945
Cl	0.011395[c]	0.016698[d]	0.01585[e]
C	0.184	0.04192	0.12758
N	0.00157[f]	0.00149[f]	0.00147[f]
H	3.263	0.7207	2.179448
O	29.6665	30.7216	31.13762

Note. We used data on chemical composition of igneous rocks of ore-bearing structures in the central Okhotsk-Chukchi volcanogenic belt published in [47–52]; n, number of specimens.

[a] Maximum mean (n = 20) in granitoids of the Turomcha volcanotectonic structure.

[b] Maximum mean (n = 60) in rhyolites and rhyodacites of the Omsukchan volcanotectonic structure.

[c] Andesites of the Omsukchan structure (n = 40).

[d] Rhyolites and rhyodacites of the Omsukchan structure (n = 60).

[e] Granitoids of the Omsukchan structure (n = 10).

[f] After Vinogradov [83].

magma chamber, which is accompanied by intense degassing and transport of fluids to the zone of surface circulation and discharge. This is a stage of active degassing. After the melt has been crystallized by more than 50%, the intensity of fluid flow drastically decreases. Supply of the fluid to the hydrothermal system decreases by a factor of about five. This is the second, longer, stage of passive degassing of a deep-seated source. In the nonconvective stage the rate of discharge of the deep source is reduced to 500 tons/day ($2\cdot10^5$ tons/year) and even to 82.2 tons/day ($3\cdot10^4$ tons/year), which is close to the flow rate of low-temperature fumarole sources in passively discharging volcanic systems [30, 37, 38].

We assume that the mass flow of fluid from a deep-seated source is equal to $5.2\cdot10^5$ tons/year as converted to pure water. According to Shihonara and Hedenquist [37], this flow can be provided by a rising andesite intrusive 100 km^3 in volume, with the starting content of water of 3.5%. Given that the efflux of fluid takes 1% H_2O, with 2.5% remaining in the solidified rock in the bounded form, the total amount of water released from the intrusive body of andesite will be equal to $2.7\cdot10^9$ tons. This amount can be supplied to the hydrothermal system by a flow of $5.2\cdot10^5$ tons/year.

In our model, the duration of action of flow of $5.2\cdot10^5$ tons of water a year is accepted to be 2000 years. This is the duration of the short stage of degassing of deep-seated source in the model by Shihonara and Hedenquist [37]. Thus, the total amount of H_2O removed from a deep-seated peripheral source in the short stage through a fractured fluid channel will be $1.04\cdot10^9$ tons, i.e., 2.6 times as low as the potential mass of runoff, which can provide an andesite asthenolith 100 km^3 in volume, from which 1% H_2O migrates during

its floatation to the submineral zone of gold-ore deposits. It is pertinent to note that in general the complex of problems connected with processes of separation of volatiles during the rise, cooling, and crystallization of deep-seated hot fluidized bodies in various structural-dynamic settings needs additional goal-oriented investigations from the viewpoint of generalization and systematization of abundant geological and geophysical data as well as in the context of physicochemical modeling. Despite the evident progress in this direction [1, 31, 36–48], a number of principal questions connected with the physicochemical nature of magmatogenic-hydrothermal systems remain open. Their solution is one of the top-priority problems of modern geochemistry.

Meteoric water flow. Under the conditions of a moderately wet climate with annual precipitation of 1250 mm, 0.125 l of rain water penetrates through 10 cm^2 of the area of geothermal block. It is supposed that the underground infiltration runoff equals 10% of the meteoric water flow. Then the amount of meteoric water penetrating across the section of hydrothermal block is equal to $4000 \times 4000 = 16{,}000{,}000$ m^2 depthward through disintegrated channels will be $2 \cdot 10^6$ m^3, or $2 \cdot 10^6$ tons. This is commensurate with the estimate of the flow of infiltration waters in the geothermal system of the island of Sutsuma Ivojima within $2-3.2 \cdot 10^6$ tons/year, i.e., 10% of annual precipitation of $25-40 \cdot 10^6$ tons/year over the area of about 20 km^2 [38].

CHEMICAL COMPOSITION OF INPUT FLOWS

The hydrothermal system is affected by two external flows: ascending – fluids from a deep-seated source, and descending – meteoric infiltration waters penetrating from the zone of transition from hydrostatic to lithostatic pressure.

To estimate the potential composition of ascending flow, we assume that the deep-seated fluid forms under the conditions of thermodynamic equilibrium with enclosing rocks in the transcritical region. Table 2 lists compositions of hydrothermal fluid resulting from water-andesite and water-rhyolite interactions at 600 °C, 1000 bars and 400 °C, 450 bars, i.e., below the boundary of transition (see Fig. 1) from hydrostatic to lithostatic pressure.

As initial compositions of rocks we took data from Table 1. Support for thermodynamic rock-water equilibrium in the high-temperature region >300 °C comes from analyses of hot waters from the wells drilled in the hydrothermal system of Baransky Volcano (Iturup Island, the Kuriles) [42]. Table 2 also reports compositions of pure rain water thermodynamically equilibrated with the atmosphere (15 °C, 1 bar) and the hydrothermal solution obtained as a result of rain water-andesite interaction in a continuous megasystem of reservoirs 1, 2, and 3 (see Fig. 1) after the completion of the 32nd cycle (see below). The water saturated with atmospheric gases is considered an initial infiltration flow of meteoric origin.

Basic multisystem. The number of independent components, including electron (e), is equal to 16: K-Na-Ca-Mg-Fe-Al-Si-Au-Ag-S-Cl-C-N-H-O-e. The list of substances which can potentially be in equilibrium consists of 155 dependent components of aqueous solution, including the H_2O solvent itself, 14 gases, and 35 mineral phases. Necessary thermodynamic information was taken from the Selektor-C-integrated database SPRONS92/DAT [6, 9, 49–54]. The parameters of a modified HKF equation of state [3–5] for HCl^0, a dependent component of the aqueous solution, are taken from [55] and for $AuHS^0$ are calculated using the algorithm from [10], and the thermodynamic characteristics of gases are taken from [56]. Individual characteristics of activity of ions and neutral complexes γ_j are calculated from a modified Debye–Hückel equation [3, 5]. Coefficients of fugitivity and molar volumes of gases were calculated from three-parameter [57] and two-parameter [58, 59] equations of state. The compositions of solid solutions of Au-Ag, carbonate, chlorite, amphibole (tremolite-actinolite), light mica (muscovite-paragonite), and biotite (annite-phlogopite) were calculated from an ideal model. The conventional term "light mica" needs some explanation. At present, satisfactory estimates of thermodynamic properties of illites (sericites) and hydromicas (including hydromuscovite) are made in the low-temperature domain, chiefly, with respect to supergene processes. The available definitions of thermodynamic properties of illites and hydromicas in the region of higher temperatures require additional testing and matching with thermodynamic properties of components of aqueous solution in the SPRONS system. Therefore, here we will use the conventional term "light micas", which are simulated by the solid ideal solution muscovite-paragonite.

CONTROL PARAMETERS OF IMITATION MODEL FOR HYDROTHERMAL MEGASYSTEM

Interaction of flows and enclosing rocks of a hydrothermal system can be portrayed as a set of connected reservoir systems (see Fig. 1). Meteoric precipitations form a descending infiltration flow. In the subsurface

Table 2

Molal Amounts of Independent Components in the Fluid Resulting from Thermodynamic Equilibrium in Rock-Water System

Independent component	1 kg of andesite + 0.1 kg H_2O, 600 °C, 1000 bars	1 kg of andesite + 0.01 kg H_2O, 600 °C, 1000 bars	1 kg of rhyolite + 0.01 kg H_2O, 600 °C, 1000 bars	1 kg of rhyolite + 0.02 kg H_2O, 600 °C, 1000 bars	1 kg of rhyolite + 0.1 kg H_2O, 600 °C, 1000 bars	1 kg of andesite + 0.02690 kg H_2O, 400 °C, 450 bars	1 kg of rhyolite + 0.03221 kg H_2O, 400 °C, 450 bars	Nonmineralized rain, 15 °C, 1 bar	Hydrothermal solution of meteoric origin, 350 °C, 405 bars
	1	2	3	4	5	6	7	8	9
K	2.865e-02	1.064e-01	3.892e-01	2.164e-01	4.876e-02	2.554e-02	1.099e-01		$1.193 \cdot 10^{-3}$
Na	6.797e-02	2.547e-01	9.057e-01	5.146e-01	1.160e-01	2.457e-01	4.129e-01		$4.727 \cdot 10^{-3}$
Ca	9.548e-06	1.451e-04	2.058e-03	5.682e-04	2.675e-05	1.545e-03	2.728e-03		$4.733 \cdot 10^{-6}$
Mg	3.150e-08	2.283e-07	3.881e-05	5.646e-06	3.214e-07	1.502e-07	1.020e-07		$2.445 \cdot 10^{-9}$
Fe	8.875e-06	1.550e-04	1.372e-02	4.259e-03	1.475e-04	1.344e-05	1.607e-05		$2.318 \cdot 10^{-7}$
Al	2.555e-03	2.305e-03	2.400e-03	2.494e-03	2.632e-03	9.394e-05	1.204e-04		$7.299 \cdot 10^{-5}$
Si	3.820e-02	3.503e-02	3.598e-02	3.742e-02	3.922e-02	1.721e-02	1.732e-02		$1.476 \cdot 10^{-2}$
Au	1.278e-06	4.893e-06	1.227e-05	3.581e-06	2.647e-07	3.495e-07	1.619e-06		$< 10^{-10}$
Ag	3.125e-05	1.197e-04	3.018e-04	1.684e-04	3.702e-05	6.764e-05	1.148e-04		$4.317 \cdot 10^{-9}$
S	4.977e-01	1.684e+00	8.747e-01	4.878e-01	1.074e-01	3.755e-02	3.570e-02		$1.14 \cdot 10^{-2}$
Cl	9.375e-02	3.589e-01	1.327e+00	7.398e-01	1.628e-01	2.740e-01	5.277e-01		$< 10^{-10}$
C	1.514e+00	5.794e+00	3.331e+00	1.857e+00	4.088e-01	2.003e+00	1.324e+00	1.598e-05	$1.01 \cdot 10^{-2}$
N	1.292e-02	4.945e-02	1.184e-01	6.602e-02	1.453e-02	3.776e-02	4.709e-02	1.436e-03	$1.436 \cdot 10^{-3}$
H	113.105	115.755	114.657	113.599	112.002	111.09702	111.09275	111.0200046	111.03747
O	58.607	56.665	62.077	59.242	56.411	59.551	58.195	55.5106744	55.56797
W/R	0.1372	0.0438	0.0159	0.026	0.107	0.04426	0.0346		
pH	7.48	7.21	6.41	6.59	6.94	6.25	6.384	5.63	7.24
Eh	–0.903	–0.856	–0.73	–0.76	–0.797	–0.473	–0.485	0.896	–0.5496
lgP_{O_2}	–19.75	–20	–20.2	–20.07	–19.4	–25.776	–25.595		–28.074
H_2O, %	12.06	4.2	1.57	2.54	9.6	4.47	3.35		

zone of free water exchange it is mixed with the discharge flow of deep-seated melts and successively, from top to bottom, passes through three reservoirs numbered 1, 2, and 3. These three reservoirs represent a tripartite massif of the enclosing rocks of a hydrothermal building. The volume of each reservoir is $2 \cdot 10^9$ km^3, and the mass, $5.4 \cdot 10^9$ tons. Thus, the model for interaction of meteoric infiltration waters with the enclosing rocks of the hydrothermal system takes into account as little as a fourth part of the whole deconsolidated block. In other words, the descending flow of meteoric waters does not cover the entire volume of the enclosing rocks. Infiltration runoffs are localized in zones with relatively high permeability, which alternate with sites of hindered permeability. As shown above, the mass of the annual infiltration runoff is $2 \cdot 10^6$ tons of H_2O a year.

Subdivide the functioning of the hydrothermal system into 32 cycles (periods). If the total duration of functioning of "hydrothermal kettle", including a short stage of active degassing plus a stage of passive degassing, is equal to 12,000 years, then one cycle will last 375 years. Then the mass of input infiltration flow entering the 1st reservoir will be $7.5 \cdot 10^8$ tons of H_2O a cycle. Given below are the main parameters of reservoirs 1 to 3 (Table 3). Depth, temperature, and pressure are determined at the central point of each reservoir and are extrapolated onto the whole volume. It is noteworthy that the pressure in reservoirs 1, 2, and 3 exceeds the pressure in a through-flow fractured channel (in reservoirs 4 to 12) at one section in depth.

Table 3

Reservoir	Depth, km	T, °C	Pressure, bars	Initial mass of rocks, tons	Mass of runoff of infiltration waters for one cycle, tons
1	0.5	100	135	$5.4 \cdot 10^9$	$7.5 \cdot 10^8$
2	1.0	250	270	»	Determined in the process of modeling
3	1.5	350	405	»	The same

This "specified" excessive difference models conditions in real systems fractured zone–enclosing rocks, which provide the flow of hydrothermal solutions through channels and which hinder pumping of an endogenous fluid from channel to enclosing rocks.

The ascending flow of deep-seated fluids through the fractured zone is simulated by nine reservoirs, 4th to 12th (see Fig. 1). A deep-seated chamber is discharged through them for 2000 years at the rate of $5.2 \cdot 10^5$ tons of H_2O a year as recalculated to pure water. The width of the fractured fluid channel is 20 m; length, 4000 m; extension depthward, 1500 m; volume, $12 \cdot 10^7$ m^3; and initial mass, $32.4 \cdot 10^7$ tons. The density of the fractured fluid channel is supposed to be 2.7 tons/m^3. The initial mass of each of the reservoirs 4–12 equals $3.6 \cdot 10^7$ tons. The main parameters of reservoirs 4 to 12 (Table 4) are characterized by the following figures (geobarotherm):

Table 4

Parameter	Reservoir no.								
	4	5	6	7	8	9	10	11	12
Depth, km	1.5	1.25	1.2	1.05	0.9	0.7	0.5	0.3	0.1
T, °C	350	325	300	275	250	225	200	150	100
Pressure, bars	261.4	126.4	121.0	107.1	94.4	74.6	54.6	35.6	11.6

The reported figures show that the geobarotherm follows the path where the pressure exceeds the water saturation pressure. The initial mass of ascending deep flow for one cycle is equal to $3.25 \cdot 10^7$ tons/cycle. The whole 2000-year lifetime of an intense deep-seated flow is subdivided into 32 cycles. One cycle includes 62.5 years. The rate of filtration in the fractured zone is supposed to be higher than the rate of descending infiltration of meteoric waters in the massif of enclosing rocks. If the volume of infiltrated meteoric rocks for the whole period of existence of the hydrothermal system (12 ka) is supposed to be equal to $2.4 \cdot 10^{10}$ m^3 and the area of the cross section of filtration in the enclosing rocks is 4 mln m^2 (1/4 of the entire cross section of the hydrothermal block), the velocity of infiltration flow will be about 0.5 m/year or 187.5 m for a 375-year cycle.

For 2000 years, the amount of fluid percolated from a deep-seated source is $1.04 \cdot 10^9$ m^3 recalculated to pure water. The area of the cross section of the fractured channel is $20 \times 4000 = 80{,}000$ m^2. Then the rate of effusion of the deep stream will be about 6.5 m/year. It takes 230 years, or 3.68 cycles (one cycle is 62.5 years), for a deep stream to pass the entire 1.5 km conduit connecting the "bottom" of the hydrothermal system with the surface. Thus, the portion of the 1st cycle hydrothermal solution reaches the depth of the fourth root reservoir for 3000 years, or for eight 375-year cycles, i.e., after the completion of the first stage, when the ascending deep fluid rises through the stem flow-through zone.

Realization of the model. In this paper we will restrict ourselves to solving only one problem. Using an imitation model, we will try to answer the question about the main source of gold and mechanisms of its concentration in ore zones of epithermal Au-Ag deposits of the Eveny zone of the Okhotsk-Chukchi volcanic belt. The dynamic model of the megasystem of hydrothermal building will be realized according to the algorithm of successive interaction, the second algorithm described by Chudnenko et al. [2].

We will consider several "limiting" scenarios of possible development of processes of dissolution, transport, and deposition of gold (in the form of Au-Ag solid solution) in the framework of those assumptions and restrictions which are specified in the above data; composition of flows connecting 12 reservoirs of

hydrothermal megasystem; dimensions of the hydrothermal prism; lifetime and rate of running, filtration, and infiltration of flows of water solutions.

Scenario 1. It implies the rise of a deep-seated fluid obtained from the thermodynamically equilibrium andesite-water interaction in a submineral zone at 400 °C and 450 bars. Hereafter, this starting fluid will be called fluid-6 (according to its number in Table 2). For comparison, Table 2 lists compositions of possible initial fluids that formed in the submineral zone under the conditions of thermodynamic equilibrium (600 °C, 1000 bars; 400 °C, 450 bars) with andesite and rhyolite containing varying contents of H_2O and, therefore, having varying rock-water ratio (R/W). Data from Table 2 are rather illustrative. In the submineral zone, under supercritical conditions in the ranges 400–600 °C, 450–1000 bars, gold and silver are significantly redistributed from rock to fluid phase. As compared with rock, the content of gold in fluid increases by a factor of 200 to 500, and of silver, 100 to 200. The main dependent component of gold in solution is hydrosulfide $Au(HS)_2^-$. Chloride complexes of Au are subordinate, no matter which rock is in thermodynamic equilibrium, andesite or rhyolite. Silver is transferred by both chloride and hydrosulfide complexes, with the chloride ones being predominant in "rhyolite" fluids. The initial R/W of fluid-6 is 22.59, which corresponds to 4.47% H_2O in andesite (see Table 2). According to Fyfe et al. [60], this is a fluid formed in the "rock-dominated" regime of rock-water interaction.

Scenario 1 is appropriate to model the ascending flow of fluid-6 through reservoirs 4–6 without interaction with the enclosing rock. The aqueous solution and forming gases are transported through a chain of reservoirs as a single group of mobile phases [2]. Scenario 1 model permits us to estimate the potential possibility of transport and deposition of Au from a deep-seated fluid only at the cost of a successive decrease in temperature and pressure, which in our case is higher than the H_2O saturation pressure over the whole geothermobarometric path. This scenario is possible under real conditions when the deep-seated fluid rises from bottom to top through high-permeability zones with insignificant chemical interaction with the enclosing rocks. The free passage of fluid seems to be of low probability at early, initial stages of existence of hydrothermal megasystem, when the subsystem of fluid and subsystem of enclosing rock are thermodynamically inconsistent. But later, the fluid flow comes to the state close to thermodynamic equilibrium with the interacting rock, and Scenario 1 (call it conventionally the "pipe" scenario, i.e., model for free flow of fluid through well-permeable through-flow channels) becomes quite possible, especially in open fractures in near-surface zones.

Simulation according to Scenario 1 has shown that gold does not settle down in reservoirs 4 to 6. The bulk of high-fineness gold (more than 95%) is deposited in the 7th reservoir: 9.28 tons for 32 cycles. Small amounts are accumulated in the 8th, 9th, and 10th reservoirs: 0.08, 0.28, and 1.42 tons, respectively. A typical feature of Scenario 1 is that the greatest concentration of gold is mineralogically associated with zones that abound in light micas (about 90 wt.%) with a small admixture of sulfides (pyrite and argentite) and quartz. In the uppermost, 11th and 12th, reservoirs Au is not deposited. There are barren quartz veins with a small admixture of pyrite and hydromica. In the lower 4th to 6th reservoirs gold does not precipitate either. "Pure" quartz veins with insignificant admixtures of pyrite and light mica form there.

Given $5.2 \cdot 10^5$ tons of H_2O are removed from a deep-seated source each year, the runoff for 32 cycles (2000 years) will total $1.04 \cdot 10^9$ tons, i.e., theoretically 71.5 tons of gold may be carried out with the deep-seated fluid through the main through-flow channel (reservoirs 4 to 12). This estimate is not too high. A great potential gold capacity of the fluids formed under deep conditions as a result of rock-water interaction is also supposed by Gammons and Williams-Jones [61] as well as by Krupp and Seward [62].

Thus, according to scenario 1, simple deposition of Au from a deep-seated fluid which does not interact with the surrounding rocks and follows the geobarotherm route to penetrate from the root zone to the zone of dissipation where a higher-than-H_2O-saturation pressure is retained, leads to accumulation of this metal for about 15% of its amount carried out by the flow of deep-seated fluid.

The mechanism of deposition according to Scenario 1 is rather simple. This is the redistribution of sulfide sulfur of aqueous solution, including the sulfide sulfur from the main form of Au occurrence in solution, hydrosulfide complex $Au(HS)_2^-$. The sulfide sulfur is partly consumed to form sulfides (pyrite, argentite) and partly transforms into a gas phase in the form of H_2S and SO_2. The concentration of hydrosulfide complex $Au(HS)_2^-$ decreases, and gold precipitates in the form of solid solution containing more than 70% Au. Thus, gold deposition is governed by redistribution of sulfide sulfur into solid and gas phases, which leads to some increase in Eh and decrease in pH of aqueous solution. Distribution of Eh and pH over reservoirs after the 32nd cycle has been completed is characterized by the following figures: 4 – 0.32, 5.3 (hereafter, the first digit stands for the number of reservoir, the second, Eh, and the third, pH); 5 – 0.24, 5.1; 6 – 0.25, 4.9;

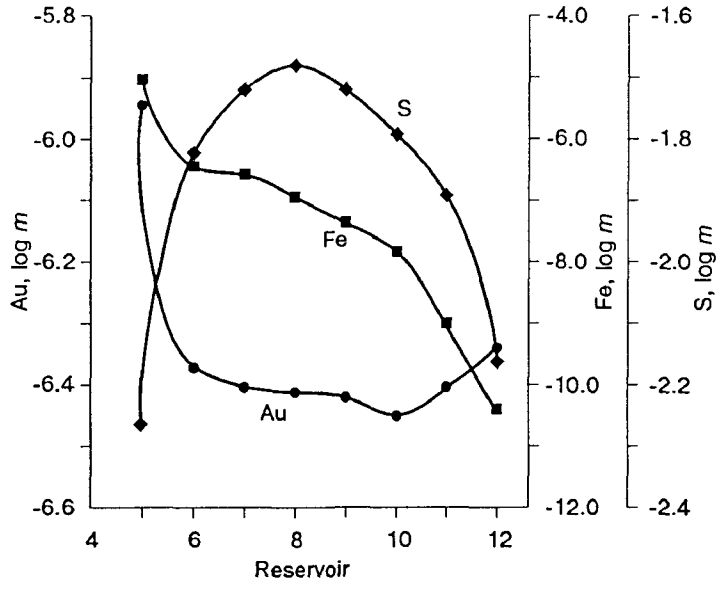

Fig. 2. Distribution of Au, S, and Fe (m – molality) after the completion of the 32nd cycle in the model for rise of a deep-seated fluid through the main channel wihout interaction with enclosing rocks. The rising flow follows the geobarotherm with a pressure exceeding the water-saturation pressure.

7 – 0.2, 4.5; 8 – 0.18, 4.3; 9 – 0.15, 4.2; 10 – 0.13, 4.2; 11 – 0.08, 4.1; 12 – 0.06, 4.0. Despite increased Eh, gold is not deposited in the upper reservoirs. There, considerably smaller amounts of sulfide sulfur are redistributed from aqueous solution to solid phase (pyrite) because of iron exhaustion in previous reservoirs, and, although sulfide sulfur continues to separate into the gas phase, the solution becomes undersaturated in metallic Au, although its concentration somewhat increases. The pattern of distribution of Au, S, and Fe as well as Eh and pH in solution after the termination of the 32nd cycle in the model of ascending deep-seated fluid through the main conduit without interaction with the host rocks is schematically shown in Fig. 2. The "pipe" model is important as it explains the formation of "auriferous" micaites (of the light micas, sericite and hydromuscovite) deposited in open cracks and substituting for feldspars, as well as the potential possibility of "supply" of gold in the form of hydrosulfide complexes from a deep-seated source to the near-surface zone of spreading and discharge.

Scenario 2. Simulated degassing. A deep-seated fluid from the root zone of contraction of hydrotherms penetrates through the main fractured zone in the flow-through regime along the geobarotherm without interaction with the surrounding rocks, but in the range of 100–200 °C in the upper reservoirs the pressure drops to H_2O-saturation pressure, which leads to outboiling of the hydrothermal solution. This is a "boiling" model.

Numerical experiments show that theoretically, under the conditions of stationary degassing of the ascending flow, all Au amounting to 70 tons might have been deposited in the first (as the hydrothermal solution moves) reservoir in which the pressure falls down to H_2O-saturation pressure. The mineral composition of solid phases is nearly pure quartz with highly fine (>97%) gold. Therefore, if the discharge of hydrothermal flow proceeds according to Scenario 2, the appearance of gold-bearing quartz veins is quite possible. The mechanism of gold deposition according to the second scenario is redistribution of sulfide sulfur from aqueous solution to gas phase.

Scenario 3. A model for mixing with meteoric water. An endogenous fluid moves up the geobarotherm and, beginning with the 8th reservoir, is mixed with meteoric waters, saturated with atmospheric oxygen. The meteoric water was rain water brought to thermodynamic equilibrium (15 °C, 1 bar), whose composition is given in Table 2. Mixing occurs without interaction with the enclosing rocks. As a result of mixing of meteoric waters with a deep-seated fluid, pH decreases, Eh increases, and metallic gold is deposited. Figure 3 shows its total amount deposited after the completion of the 32nd cycle as a result of interaction between meteoric waters, MW, and deep-seated fluid, DF, depending on MW/DF expressed in weight units. The total includes

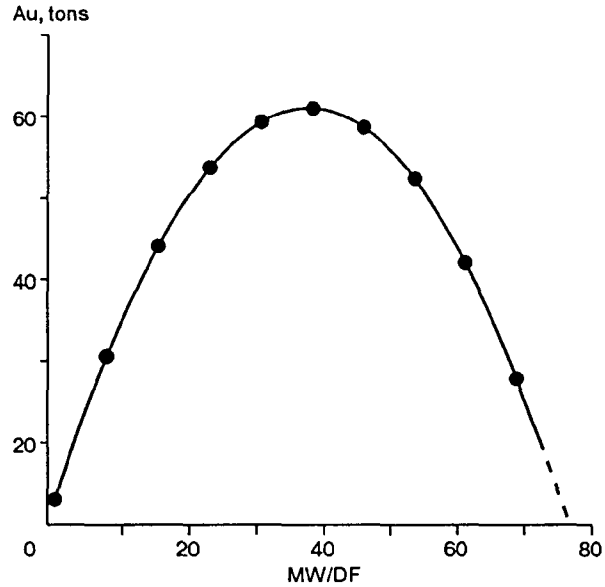

Fig. 3. The total amount of gold deposited after the completion of the 32nd cycle as a result of mixing of meteoric waters, MW, and a deep-seated fluid, DF. For explanation see the text.

the gold deposited in the 7th reservoir according to Scenario 1 – about 9 tons. Mixing begins with the 8th reservoir. The behavior of pH and Eh in the 8th reservoir depending on MW/DF is illustrated in Fig. 4.

The process of mixing is accompanied by increased Eh and decreased pH. But the amount of deposited Au depends on MW/DF. The optimal MW/DF values are in the range 10 : 1 to 60 : 1. Given less oxidant, the effect of dilution does not exert a considerable effect on Au concentration. And, vice versa, too strong dilution leads to the situation when the mixed solution becomes undersaturated with native metal. It is important to stress that dilution hinders gas release. Therefore, gold deposition according to Scenario 3 is not related to fractionation of sulfide sulfur from solution to gas phase. In this case, mainly the mechanism works which involves oxidation of sulfide (if MW/DF $\leq$ 1) sulfur to sulfate one and, partially, binding of sulfur from aqueous solution to form sulfides. The fineness of the gold formed according to Scenario 3 is more than 90%. The higher MW/DF, the higher the content of pure gold, up to 96% Au and 4% Ag. Of special importance is that, according to Scenario 3, when MW/DF $\geq$ 10, gold settles down in the form of a single phase, without admixture of other mineral phases, quartz and sulfides.

Scenario 4. A model for interaction of deep fluid with enclosing rocks. The deep fluid running through the main fractured zone along the geobarotherm interacts with andesite (see Table 1) according to a scheme of simple succession with the input to the 4th reservoir and output from the last, 12th, reservoir into the zone of discharge and spreading, i.e., the model for through-flow megasystem [2]. The total consumption of deep-seated fluid for 32 cycles (2000 years), as noted above, is $1.04 \cdot 10^7$ tons of fluid recalculated to solvent, pure water. The mass of the fractured zone is $3.28 \cdot 10^8$ tons. Given the consumption of deep-seated fluid in one cycle is $3.6 \cdot 10^7$ tons, the initial ratio is $R_0/W_0 \approx 0.9$. We report these figures as the marking reference, because in model experiments different initial ratios R_0/W_0 were specified, from 0.1 to 10. This range imitates either a possible expansion or contraction of fractured channel within 2–200 m, when W_0 = const, or increase-decrease of flow, when R_0 = const. In the process of ascending flow of fluids through the fractured channel and its interaction with enclosing rocks, as temperature and pressure fall, H_2O is partly removed from rock and partly used to form water-bearing minerals – light micas (sericite, hydromuscovite), biotite, chlorite, epidote, and actinolite. Current R/W in reservoirs 4 to 12 will change from cycle to cycle. Numerical experiments show that in each model throughout the 32 cycles in reservoirs 4 to 12 the initial R_0/W_0 deviates by a factor of 1.5–3 toward larger and 1.5 toward smaller values. These fluctuations are related to the release or absorption of water in the process of formation of anhydrous or hydrous minerals. Figure 5 shows Au accumulation in the fractured zone after the completion of the 32nd cycle as a function of R_0/W_0 in reservoirs 7, 8, and 9. As

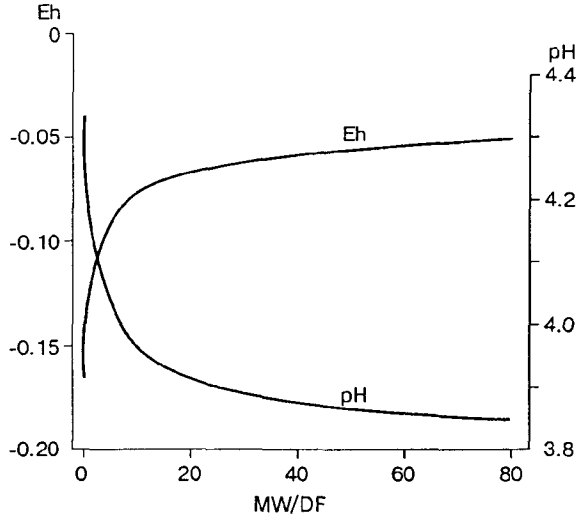

Fig. 4. Behavior of pH and Eh in the model of mixing. The plot shows pH and Eh values in the 8th reservoir after the completion of the 32nd cycle. MW/DF are given in weight units.

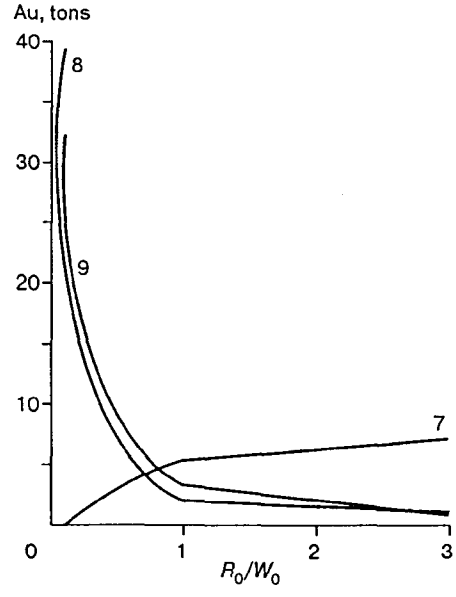

Fig. 5. Amount of gold deposited in fractured channel as a result of deep-seated fluid–andesite interaction in reservoirs 7, 8, and 9 as a function of a given value of R_0/W_0.

R_0/W_0 decreases, the region of its accumulation moves toward higher reservoirs. Under real conditions, the decrease in R_0/W_0 can bear on the intensity of hydrothermal flow in the fractured channel, which is geologically due to the narrowing of the fluid conduit and/or simply to increased flow rate of the deep-seated source. Deposited Au is of high fineness. Silver content does not exceed 10–20 wt.%. A typical feature of Scenario 4 is accumulation of Ag at the bottom of the main channel (reservoir 5) in versions with initial $R_0/W_0 \leq 1.5$.

The chemical mechanism of gold deposition is redistribution of sulfide sulfur from complex $Au(HS)_2^-$ into newly formed solid phases – pyrite, pyrrhotite, and argentite – and quite specifically, into a gas phase with the formation of H_2S. Upward movement of gold-ore sulfur is schematically illustrated in Fig. 6, which shows the dynamics of upward displacement of the boundary of maximum precipitation of Au in separate cycles in reservoirs 5, 6, 7, and 8, with $R_0/W_0 = 0.1$. Ratio R_0/W_0 also has an effect on pH behavior in reservoirs

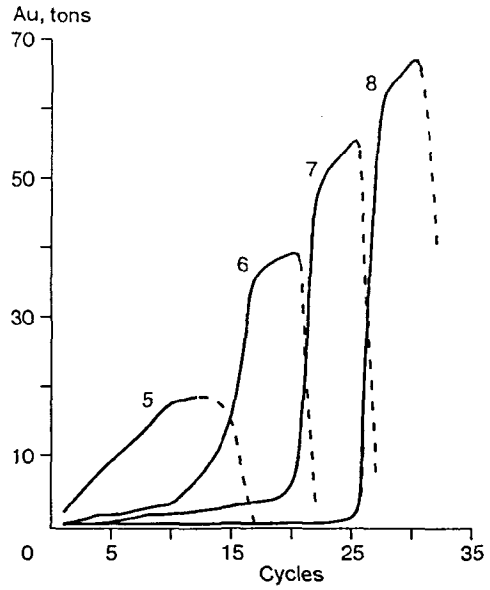

Fig. 6. Dynamics of movement of gold-ore zone from top to bottom in fractured channel as a result of deep-seated fluid–andesite interaction according to Scenario 4. 5–8, numbers of reservoirs. $R_0/W_0 = 0.1$.

of the main channel. If $R_0/W_0 < 3$, pH decreases from bottom to top, although in general the medium lies in the nearly neutral interval: $5.7 \leq \text{pH} \leq 6.1$. In models with R_0/W_0 of 3 to 10, pH increases in the upward direction from 6 to 8.

The parageneses that formed as a result of interaction of endogenous fluid-6 with andesite include minerals of the following series: quartz–light mica (sericite, hydromuscovite)–feldspars (albite, K-feldspar)–biotite–chlorite–carbonate–pyrite–magnetite–graphite–argentite–gold (Au-Ag solid solution). Depending on depth (number of reservoir) and R/W value, this list is reduced in particular model parageneses. Magnetite and chlorite are not stable in the near-surface zone of fractured channel (reservoirs 8–12) irrespective of R/W value. With decreased pH and $R_0/W_0 \leq 1$, albite decomposes to form light mica and quartz, whose amount gradually increases from bottom to top. In models with $R_0/W_0 = 0.1$, graphite begins to deposit in reservoirs 10–12. Biotite forms only in the lower zone, in reservoirs 4 to 7 in models with $R_0/W_0 \geq 1$. In general, taking into account inevitable simplifications and assumptions, the theoretical zoning is in agreement with the near-ore metasomatic zoning in andesites established by field works in the Eveny ore district in northeastern Russia [24, 27].

The following fact is noteworthy. Modeling of endogenous fluid–andesite metasomatism shows successive reduction of the number of minerals from bottom to top and, depending on R/W, the degree of rock-water interaction. But each time no more than 2–3 minerals are missing from a single metasomatic column in the direction from frontal to rear zone. Under given conditions of imitation experiments, the classical scheme of infiltration metasomatic column with a regular decrease in the number of minerals from frontal to rear zone by one or two as in models for formation of laterite beauxites, does not work [63]. The explanation is rather simple.

In our case, fluid-6 is a phase thermodynamically equilibrated with andesite in the root zone of contraction of deep-seated hydrotherms [64, 65]. When penetrating into the fractured main zone, it will be under conditions close to thermodynamic equilibrium with the enclosing rock (andesite). Therefore, a small difference in chemical potentials of independent components between the fluid and the rock to be replaced will be smoothed by the formation of as little as two or three multiphase intermediate zones. Numerical experiments with fluid-2 obtained at 600 °C and 1000 bars as a result of water-andesite interaction with $R/W = 22.81$ have shown that the mineral parageneses of metasomatite remain virtually the same as in the model with fluid-6. K-feldspar becomes more abundant, and graphite appears. Epidote and actinolite usually occur in high-temperature reservoirs 4 to 6. After the completion of the 32nd cycle, the fluid in root reservoir 4 is characterized by greater reduction in comparison with initial fluid-6.

Scenario 5. Infiltration model. It implies infiltration of meteoric waters to "root" reservoir 4 and its ascending flow through the main channel to the zone of discharge in the regime of dissipation, spreading, and mixing with meteoric waters. Table 2 compares basic parameters, including R_0/W_0, of fluid-6 and hydrothermal solution obtained as a result of modeled rain-water–andesite interaction in a total of three reservoirs 1, 2, and 3 (see Fig. 1) according to the algorithm of flow-through megasystem [2]. One cycle is 375 years.

In the water-rock system in the state of full thermodynamic equilibrium, the composition of solution and mineral paragenesis share the composition of two interacting subsystems – rock and water, which, in turn, depends on water-rock interaction. It is *R/W* ratio that determines the main thermodynamic characteristics of the system: pH, Eh, contents of independent components in solution, forms of occurrence of dissolved substances, partial pressure of gas components, and other parameters. Dependence of thermodynamic characteristics on temperature, pressure, and *R/W* is far from being evident, and many authors studied it in detail [13, 66]; so, we will not dwell on it. We only restrict ourselves to the remark that the difference in compositions of endogenous fluid-6 and hydrotherms of meteoric origin stems chiefly from differences in *R/W* rather than in temperature (450 and 400 °C) and pressure (1000 and 450 bars). But, in addition to this factor, of great importance is the prehistory of the through-flow megasystem. In particular, chlorine is rare to absent from the hydrotherm of meteoric origin because as early as first cycles of rain-water–andesite interaction chlorine is washed out from infiltration zones. Its concentration in the third reservoir first increases and then drastically decreases. Subsequent portions of infiltration waters will interact with the dechlorinated rock, and the meteoric infiltration hydrotherms contracting to the 4th root reservoir will be virtually devoid of chlorine. In our model, since cycle 10, the composition of solutions has become stable as well as the mineralogic composition of metasomatically altered andesite, transformed into propylite. The stable propylite association is quartz + light micas (sericite, hydromuscovite) + feldspars + chlorite + carbonate + pyrite. In the lower horizon (reservoir 3), epidote, actinolite, and magnetite enter this assemblage. These are typical parageneses of frontal zone of epidote propylites formed under the conditions of regional hydrothermal metamorphism within the interval 100–350 °C. The distinctive thermodynamic feature of these propylites is their multiphase nature. Each independent component of the system corresponds to a mineral phase, i.e., the number of mineral phases approximates the number of independent components, which was noticed by Gumenyuk and Gundobin [24]. Thus, within few cycles the infiltration columns feeding the 4th reservoir come to the state close to thermodynamic equilibrium with descending flow of infiltration waters, whose composition remains virtually the same throughout the period of existence of hydrothermal system. Scenario 5 does not lead to formation of Au- and Ag-bearing solutions. By the end of the 32nd cycle, the hydrothermal solution of meteoric origin contains less than 10^{-10} moles of Au in 1 kg of H_2O, and the molal concentration of Ag is $4.3 \cdot 10^{-9}$ (see Table 2). The rise of this solution through a chain of reservoirs 4–12 according to models of Scenario 1 ("pipe" model) or according to models of boiling and mixing does not provide accumulation of Au and Ag in ore zones and veins. But this conclusion is valid only in terms of the particular model considered in this work. More definite and more general conclusions can be made only on the basis of analysis of a set of models with those versions of scenarios which would answer the questions that remain beyond the scope of this paper. Analysis must be given to the processes related to the fluids that formed as a result of granodiorite-, rhyolite-, and leucogranite-water interaction as well as combined scenarios on the basis of particular geological and geochemical materials on various types of deposits. It is necessary to bear in mind that the "barren" infiltration solutions can be of critical importance in processes of remobilization, redistribution, and enrichment of Au- and Ag-bearing zones formed by endogenous fluids at early stages of the history of hydrothermal deposits.

It is most likely that the hydrothermal solutions of meteoric origin, passing along the through-flow channels from bottom to top, will transport gold and silver from the lower to the upper horizons. This process of secondary enrichment is not considered in this work. A separate problem is the model for closed and open circuits of hydrothermal currents and a series of other scenarios. But the tentative volume of studies that would be sufficient to answer these questions in the context of simulation technology can be implemented in the framework of a special program of individual project.

CONCLUSIONS

Using simulation experiments, we have studied the simplest possible scenarios of passing of fluids through permeable zones and channels in a hydrothermal system. We modeled idealized limiting versions of physicochemical interaction in a dynamic megasystem: flows of hydrothermal solutions – enclosing rocks. Although we consider each scenario independently of the rest, they all play an important role in the context

of searching for an answer to the questions posed in the Introduction to this paper: What is the source of Au during the formation of epithermal Au-Ag deposits? How does it accumulate in ore zones?

The deep-seated andesite asthenolith 50–100 km^3 in volume with an initial content of H_2O of 3.5%, floating up toward the upper horizons of ore-bearing structures of the Okhotsk-Chukchi volcanic belt (3–6 km from the surface), can provide the origin and development of a hydrothermal building extending for 1.5 km depthward in the above-chamber prism of disintegration, shattering, and fracturing in the enclosing rocks. Losing on floating up 1% water, the asthenolith forms a flow of fluids ascending through permeable channels from the root zone of contraction of hydrotherms to the near-surface zone of their spreading and discharge. Potential resources of this flow are large enough to form, under favorable geological and geochemical conditions, deposits of gold with reserves of 10–100 tons.

At the same time, the meteoric waters that percolate through andesites to the root zone of the hydrothermal block and then ascending through fractures to the surface cannot be a potential source of Au in epithermal deposits. But Au-free hydrotherms of meteoric origin may participate in redistribution and remobilization of predeposited Au and favor carrying it to the surface at the final stage of functioning of the hydrothermal system, when the flow of deep-seated fluids begins to exhaust.

The main solvent carrier of Au is $Au(HS)_2^-$. Chloride complexes of Au are subordinate irrespective of which rock is in equilibrium, andesite or rhyolite. Gold occurs in the form of both chloride and hydrosulfide, with chlorides being predominant in the rhyolite fluid.

This work was supported by grants 98-05-65303, 99-05-65667, 99-05-64487, 00-05-64377, and 00-05-64703 from the Russian Foundation for Basic Research and by grant 35 from the Siberian Branch of the Russian Academy of Sciences.

REFERENCES

[1] V. N. Sharapov, *Development of endogenous fluid ore-forming systems* [in Russian], Novosibirsk, 1992.

[2] K. V. Chudnenko, I. K. Karpov, S. I. Mazukhina, et al., *Reservoir dynamics for megasystems in geochemistry: formation of base models of processes and algorithms for simulation,* Geologiya i Geofizika (Russian Geology and Geophysics), vol. 40, no. 1, p. 45(43), 1999.

[3] H. C. Helgeson, D. H. Kirkham, and G. C. Flowers, *Amer. J. Sci.*, vol. 281, p. 1249, 1981.

[4] G. C. Tanger and H. C. Helgeson, *Amer. J. Sci.*, vol. 288, no. 1, p. 19, 1988.

[5] E. L. Shock, E. H. Oelkers, J. W. Johnson, et al., *J. Chem. Soc. London Faraday Trans.*, vol. 88, p. 803, 1992.

[6] J. W. Johnson, E. H. Oelkers, and H. C. Helgeson, *Computers Geosci.*, vol. 18, p. 899, 1992.

[7] E. L. Shock and C. M. Koretsky, *Geochim. Cosmochim. Acta.*, vol. 57, p. 4899, 1993.

[8] E. L. Shock, *Amer. J. Sci.*, vol. 295, p. 496, 1995.

[9] E. L. Shock, D. C. Sassani, M. Willis, and D. A. Sverjensky, *Geochim. Cosmochim. Acta*, vol. 61, no. 5, p. 907, 1997.

[10] D. A. Sverjensky, E. L. Shock, and H. C. Helgeson, *Geochim. Cosmochim. Acta*, vol. 61, no. 7, p. 1359, 1997.

[11] D. V. Grinchuk, E. E. Abramova, and A. V. Tutubalin, *Geologiya Rudnykh Mestorozhdenii*, vol. 40, no. 1, p. 3, 1998.

[12] M. V. Borisov and Yu. V. Shvarov, *Geokhimiya*, no. 2, p. 166, 1998.

[13] B. N. Ryzhenko, V. L. Barsukov, and S. N. Knyazeva, *Geokhimiya*, no. 12, p. 1227, 1997.

[14] D. A. Kulik, K. V. Chudnenko, and I. K. Karpov, *Geokhimiya*, no. 6, p. 856, 1992.

[15] I. K. Karpov, K. V. Chudnenko, V. A. Bychinskii, et al., *Free energy minimization in calculation of heterogeneous equilibria*, Geologiya i Geofizika (Russian Geology and Geophysics), vol. 36, no. 4, p. 3(1), 1995.

[16] I. K. Karpov, K. V. Chudnenko, and D. A. Kulik, *Amer. J. Sci.*, vol. 297, no. 9, p. 767, 1997.

[17] V. I. Sinyakov, *Fundamentals of ore genesis theory* [in Russian], Leningrad, 1987.

[18] N. V. Petrovskaya, *Native gold* [in Russian], Moscow, 1973.

[19] V. F. Belyi, *Stratigraphy and structures of Okhotsk-Chukchi volcanogenic belt* [in Russian], Moscow, 1977.

[20] M. I. Terekhov, *Stratigraphy and tectonics of the southern Omolon Massif* [in Russian], Moscow, 1979.

[21] R. B. Umitbaev, *Okhotsk-Chaun metallogenic province* [in Russian], Moscow, 1986.

[22] D. S. Korzhinskii, *Physicochemical principles of mineral parageneses analysis* [in Russian], Moscow, 1957.

[23] D. S. Korzhinskii, *Theory of metasomatic zonality* [in Russian], Moscow, 1969.

[24] V. A. Gumenyuk and G. M. Gundobin, in: *Formations of hydrothermally changed rocks and their relation to ores* [in Russian], Vladivostok, p. 84, 1978.

[25] G. M. Gundobin and R. G. Kravtsova, *Geologiya Rudnykh Mestorozhdenii*, vol. 26, no. 5, p. 49, 1984.

[26] R. G. Kravtsova, *Geokhimiya*, no. 2, p. 202, 1997.

[27] R. G. Kravtsova, *Mineralogogeochemical zonation and peculiarities of formation of gold-silver deposits in northeastern Russia*, Geologiya i Geofizika (Russian Geology and Geophyics), vol. 39, no. 6, p. 763(774), 1998.

[28] R. G. Kravtsova, *Dokl. RAN*, no. 6, p. 821, 1998.

[29] A. G. Reyes, *J. Volc. Geotherm. Res.*, vol. 43, p. 279, 1990.

[30] J. W. Hedenquist and J. R. Lowenstern, *Nature*, vol. 370, no. 6490, p. 18, 1994.

[31] W. F. Giggenbach, in: *Proceedings of the 8th International Symposium on Water-Rock Interaction: WRI-8, Vladivostok 15–19 August, 1995*, Rotterdam, p. 13, 1995.

[32] T. Shimazu, H. Matsueda, D. Ishiyama, and O. Matsubaya, *Econ. Geol.*, vol. 93, p. 303, 1998.

[33] V. Yu. Prokof'ev, *Dokl. RAN*, vol. 354, no. 1, p. 93, 1997.

[34] M. N. Zakharov, *Geochemical features of basaltoids of active continental margins (by example of the Kolyma and Koryak uplands)*, Geologiya i Geofizika (Soviet Geology and Geophysics), vol. 29, no. 6, p. 93(83), 1988.

[35] M. N. Zakharov and R. G. Kravtsova, *Geokhimiya*, no. 6, p. 507, 1996.

[36] H. Shinohara and K. Kazahaya, *Magmas, Fluids and Ore Deposits. Mineralogical Association of Canada Short Course*, vol. 23, p. 47, 1995.

[37] H. Shinohara and J. W. Hedenquist, *J. Petrol.*, vol. 38, no. 12, p. 1741, 1997.

[38] J. W. Hedenquist, M. Aoki, and H. Shinohara, *Geology*, vol. 22, p. 585, 1994.

[39] H. Shinohara, K. Kazahaya, and J. B. Lowenstern, *Geology*, vol. 23, no. 12, p. 1091, 1995.

[40] V. N. Sharapov, *To interpretation of recent endogene fluid system nature* [in Russian], Novosibirsk, 1993.

[41] V. N. Sharapov, *Phenomenological description of magmatic facies and structure-dynamic zones of magmatic systems*, Geologiya i Geofizika (Russian Geology and Geophysics), vol. 36, no. 9, p. 3(1), 1994.

[42] Yu. A. Taran, V. S. Znamenskii, and L. M. Yurova, *Vulkanologiya i Seismologiya*, nos. 4–5, p. 95, 1995.

[43] G. W. Bergantz, *Modern methods of igneous petrology: Understanding magmatic processes. Rev. Miner.*, vol. 24, p. 239, 1990.

[44] C. Jaupart and S. Tait, *Ibid.*, p. 213.

[45] S. Tait and C. Jaupart, *Ibid.*, p. 125.

[46] G. Moore, T. Vennemann, and I. S. E. Cermichael, *Geology*, vol. 23, no. 12, p. 1099, 1995.

[47] J. B. Lowenstern, *Geology*, vol. 22, no. 10, p. 893, 1994.

[48] A. F. Glazner, *Geology*, vol. 22, no. 5, p. 435, 1994.

[49] H. C. Helgeson, J. M. Delany, H. W. Nesbitt, and D. K. Bird, *Amer. J. Sci.*, vol. 278A, p. 1, 1978.

[50] R. G. Berman and T. N. Brown, *Contr. Miner. Petrol.*, vol. 89, p. 168, 1985.

[51] M. V. Chase Jr., C. A. Davles, J. R. Downey Jr., *J. Phys. Chem. Ref. Data*, vol. 14, Suppl. 1, p. 1, 1985.

[52] T. J. B. Holland and R. Powell, *J. Metamorph. Geol.*, vol. 8, no. 1, p. 88, 1990.

[53] T. J. B. Holland and R. Powell, *J. Metamorph. Geol.*, vol. 16, no. 3, p. 309, 1998.

[54] R. A. Robie and B. S. Hemingway, *U. S. Geol. Sur. Bull.*, no. 2131, 1995.

[55] B. R. Tagirov and A. V. Zotov, in: *Proceedings of the 8th International Symposium on Water-Rock Interaction: WRI-8, Vladivostok 15–19 August, 1995*, Rotterdam, p. 837, 1995.

[56] R. Reed, J. Prausnitz, and W. Sherwood, *Properties of gases and liquids* [Russian translation], Leningrad, 1982.

[57] B. I. Lee and M. G. Kesler, *AICHE J.*, vol. 21, p. 510, 1975.

[58] G. J. E. Breeveld and J. M. Prausnitz, *Thermodynamic properties of supercritical fluids and their mixtures at very high pressures (Supplementary Notes and Detailed Tables). Document 022105 of National auxiliary publications Service (NAPS)*, 1972.

[59] G. J. E. Breedveld and J. M. Prausnitz, *AICHE J.*, vol. 19, p. 783, 1973.

[60] W. Fife, N. Price, and A. Thompson, *Fluids in the Earth's crust* [Russian translation], Moscow, 1981.

[61] C. H. Gammons and A. E. Williams-Jones, *Econ. Geol.*, vol. 62, p. 45, 1997.
[62] R. E. Krupp and T. M. Seward, *Miner. Deposita*, vol. 25, p. 73, 1990.
[63] I. K. Karpov, *Physicochemical computer modeling in geochemistry* [in Russian], Novosibirsk, 1981.
[64] G. L. Pospelov, *Geologiya i Geofizika*, no. 11, p. 28, 1962.
[65] G. L. Pospelov, *Geologiya i Geofizika*, no. 12, p. 41, 1962.
[66] B. N. Ryzhenko, V. L. Barsukov, and S. N. Knyazeva, *Geokhimiya*, no. 5, p. 436, 1996.

Recommended by G. N. Anoshin

Received 21 August 2000
Accepted 14 June 2000